Sustainable Computing: Informatics and Systems 31 (2021) 100578

Contents lists available at ScienceDirect

Sustainable Computing: Informatics and Systems

journal homepage: www.elsevier.com/locate/suscom

Forecasting energy generation in large photovoltaic plants using radial belief neural network

Yuvaraj Natarajan [a,*], Srihari Kannan [b], Chandragandhi Selvaraj [c], Sachi Nandan Mohanty [d]

[a] Training and Research, ICT Academy, Chennai, 600096, India
[b] Department of Computer Science and Engineering, SNS College of Technology, Coimbatore, 641107, India
[c] Department of Computer Science and Engineering, JCT College of Engineering and Technology, Coimbatore, 641105, India
[d] Department of Computer Engineering, College of Engineering Pune, pune, India

ARTICLE INFO

Keywords:
Photovoltaic
Back propagation neural network
Restricted boltzmann machines
Radial belief neural network

ABSTRACT

Forecasting the energy generation from the solar power is considered challenging due to inaccuracies in forecasting, reliability issues and substantial economic losses in power systems. Hence, it is necessary to consider wide features from the solar power generation point of view. In this paper, the study uses large features set to feed the deep learning classifier for optimal prediction of energy generation from the photovoltaic (PV) plants. The features selection and prediction modules automates the process of optimal prediction of energy using Radial Belief Neural Network (RBNN). The Restricted Boltzmann Machines (RBM) is used for rule set generation based on the feature extracted and the rule set generation is powered by action-reward based Reinforcement Learning (RL) method. The experiments are conducted with rich set of input features on large PV plants that ranges between 1, 50, 100 and 1000. The performance of the proposed model is compared with various metrics that includes: Root mean squared error (RMSE), normalized root mean squared error (NRMSE), mean bias error (MBE), Mean absolute error (MAE), Maximum absolute error (MaxAE), mean absolute percentage error (MAPE), Kolmogorov–Smirnov test integral (KSI) and OVER metrics, Skewness and kurtosis and variability estimation metrics. The simulation results show that the RBNN offers improved prediction ability with reduced errors than other deep and machine learning classifiers.

1. Introduction

Artificial Intelligence (AI) is a computing engine that performs complex tasks than a straightforward programming [16]. It offers the ability of exploiting itself to offer a power computation. In order to produce efficient and effective computations, wide features are often necessary to interpolate the knowledge on the field [21].

Solar energy solutions are the core components of sustainable energy for a clean, green or domestic energy supply. Global solar radiation is divided into two parts: one is the diffuse solar radiation originating from the dispersion of gas in the earth's atmosphere, water droplets and particles; and the other is direct solar radiation that is not scattered. The algebraic sum of the two elements is global solar radiation. Global and diffuse radiation values are important for applications in science and engineering.

In addition to optimum site selection for solar power plants, solar radiation data are critical for their architecture, scale, service, and economic evaluation. The sizing of photovoltaic (PV) systems plays an important role. However such data, particularly in remote areas, is not always accessible. The only practical means of collecting radiation data in daily or hourly time scales is to produce synthetic solar radiation values. This is since only a handful of sites or areas are present in each country with calculated sequences of radiation values, and even when available they are typically available at various times. Several models in the study and numeric simulation were developed for the calculation of global solar radiation data, insolation and daily cleanliness index on different scales.

The existing methods [1–15,17–26,29,30] at times falls with inaccurate forecast due to increased parameters and that causes higher prediction error. Usually, these models encounter into various other problems like missing data, inaccurate forecast on long run, prediction of data based on a specific location with inaccurate measurement

* Corresponding author.
E-mail addresses: yraj1989@gmail.com (Y. Natarajan), harionto@gmail.com (S. Kannan), chandragandhi09@gmail.com (C. Selvaraj), sachinandan09@gmail.com (S.N. Mohanty).

https://doi.org/10.1016/j.suscom.2021.100578
Received 16 December 2020; Received in revised form 11 May 2021; Accepted 6 June 2021
Available online 9 June 2021

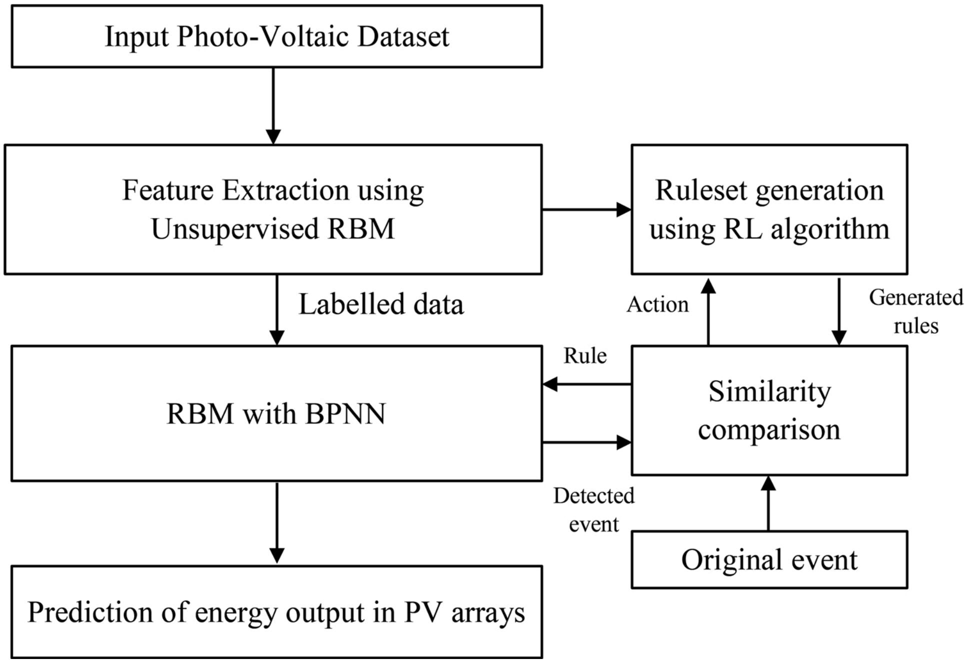

Fig. 1. Architecture of Detection using RBNN model.

devices. To resolve these problems, we adopt following metrics that includes the collection of various neural network algorithms and reinforcement learning (RL) algorithm to accommodate various features to produce reduced prediction error.

The main contribution of the paper involves the following:

- The author forms an automated prediction model with increased number of features that detects the events in an optimal way.
- The author develops a prediction model using Radial Belief Neural Network (RBNN) that consists of a combination of a Restricted Boltzmann Machines (RBM) [3,7,24] for the extraction of features and Back Propagation Neural Network (BPNN) for the classification of features [6,10,27]. The former is an unsupervised model and the latter is a supervised model.
- Further a rulesets are generated using reinforcement learning (RL) [7,13,20,28] method based on the feature extracted with action-reward model that defines the rules for prediction using the BPNN over various datasets collected from various plants to predict the performance of large PV plants.

The remainder of the paper is given below: Section 2 provides the related works. Section 3 discusses the proposed method that includes the collection of input features, data sample selection, feature extraction and data representation. Section 4 evaluates the prediction model and Section 5 concludes the entire work with possible directions for future scope.

2. Related works

Abedinia, O., et al. [1] uses 2-stage feature selection filter to improve the forecasting using neural network. The combination of metaheuristic optimization enables the learning algorithm used in the study to train efficiently the ANNs for forecasting purpose. However, the study fails at premature convergence due to the utilisation of metaheuristic solution in the search space.

Barrera, J. M., et al. [4] collected various natural factors in the environment using Internet of Thing (IoT) devices to predict the production of energy using ANN. The study achieves reduced mean square error with improved accuracy for forecasting. However, the study fails to provide the critical data for optimal training of the model. This poses the unavailability of certain critical features to train effectively the ANNs.

Mousavi, S. M., et al. [23] combined simulated annealing with ANN to forecast the daily solar radiation unto a horizontal surface. The simulated annealing effectively overcomes the problem of falling into local optimal and prevents the formation of premature solution in the search space. However, the failure in utilising certain factors like clearness index, sunshine duration, extra-terrestrial radiation and vapour pressure reduces the training and validation accuracy.

Rodríguez, F., et al. [26] develops ANN to predict the solar energy generation using the photovoltaic generators. The study predicts the parameters in order to estimate the future power production that optimises the grid control. However, the study at times fails to utilise certain parameters that are non-essential for the study and this may affect the performance of prediction of solar energy radiation.

Sun, W., & Huang, C. [27] predicts the emission of carbon dioxide using back propagation neural network. The study takes into concern most of the error metrics to check the fitness of the neural network model. Failure in considering the factors related to market behaviour affects the probable emission of CO_2 in the atmosphere and therefore the prediction accuracy is reduced.

3. Proposed method

Fig. 1 shows the model of the RBNN that consists of RBM with BPNN models. The study using RBNN is used for the prediction of events related to large PV plants performance.

3.1. Input features

In order of designing the RBNN model for predicting the sustainable solar energy in PV output, it is essential to analyse the factors associated with the generation of energy. Such factors are regarded as inputs to the BPNN and these are tailored adequately to predict the output on various situation.

The initial elements influence on forecasting the solar energy is the solar components that offers input for processing and converting into energy with a photovoltaic cell excitation, generation of solar energy

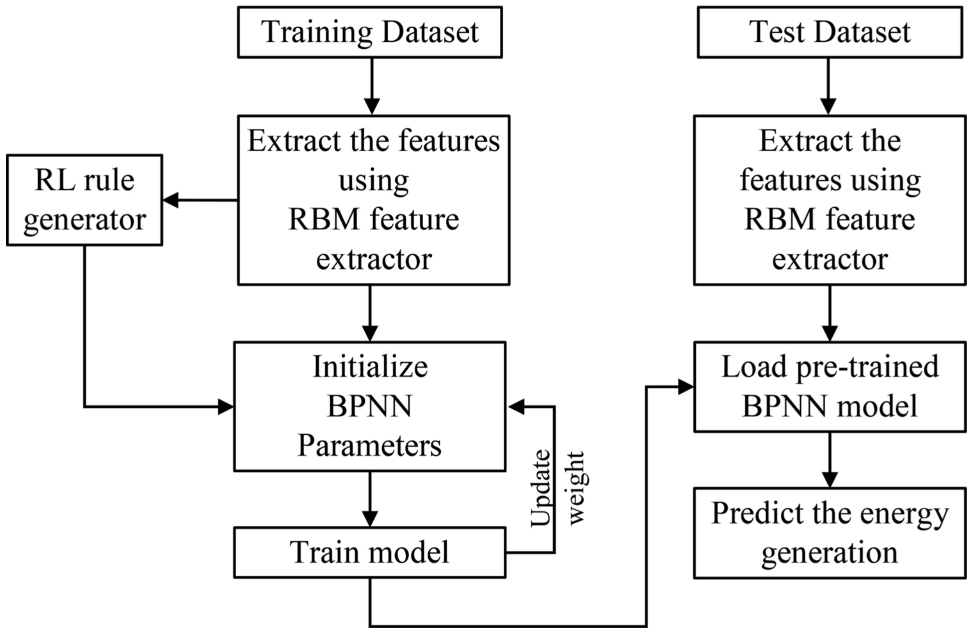

Fig. 2. Architecture of Training-Testing RBNN prediction.

Table 1
PV system specifications.

Modules	Value
System Capacity	264 – 231 kWac
Azimuth angle	36°
Tilt angle	11°
Inverter power	13 × 17 kW + 1 × 10 kW
Inverters	SMA Tripower
Solar panels type	Polycrystalline Solar Panels (Poly-SI)

Table 2a
Metrics evaluated for Next one year time period over a solar plant with 100 PV arrays using proposed RBNN and other methods.

Metrics	One hour-ahead	One-day ahead
Correlation coefficient	0.77216	0.6604
RMSE (MW)	17.39392	22.42312
NRMSE	0.17272	0.22352
MaxAE (MW)	75.51928	85.4456
MAE (MW)	11.52144	15.04696
MAPE	0.11176	0.1524
MBE (MW)	2.22504	4.33832
KSIPer (%)	106.0907	220.1977
OVERPer (%)	28.61056	138.5418
SD (MW)	40.20312	21.9964
Skewness	0.08128	−0.19304
Kurtosis	2.4384	2.07264
95th percentile (MW)	40.20312	51.39944
Capacity (MW)	101.6	101.6

from the renewable source. These components are responsible for the generation of energy from the solar panel that includes: *direct radiation, diffuse radiation and reflected radiation*. These three components forms the Global Radiation value that does not considers the angle of rays reaching the panels. This value is further used to estimate the solar radiation on tilted surface to estimate the radiation output. Various other parameters for solar energy generation depends on other factors that includes *solar azimuth angle, air temperature and wind speed*. After the solar rays reaching the panel, certain other components further influences the generation of energy in the electrical components related to photovoltaic installation that includes: *PV panel performance and PV installation size*.

Table 2b
Metrics evaluated for Next one year time period over 50 solar plants using proposed RBNN.

Metrics	One hour-ahead	One-day ahead
Correlation coefficient	0.95504	0.88392
RMSE (MW)	288.9098	445.262
NRMSE	0.08128	0.13208
MaxAE (MW)	1325.606	2297.115
MAE (MW)	194.2287	291.2364
MAPE	0.06096	0.08128
MBE (MW)	32.14624	133.9291
KSIPer (%)	53.68544	187.2488
OVERPer (%)	0.78232	95.94088
SD (MW)	287.1419	424.688
Skewness	−0.2032	0.2032
Kurtosis	2.56032	3.85064
95th percentile (MW)	647.6492	1006.511
Capacity (MW)	3518.408	3518.408

Table 2c
Metrics evaluated for Next one year time period over 100 solar plants using proposed RBNN.

Metrics	One hour-ahead	One-day ahead
Correlation coefficient	0.97536	0.92456
RMSE (MW)	384.7084	634.177
NRMSE	0.06096	0.1016
MaxAE (MW)	1763.004	3434.364
MAE (MW)	260.797	419.7198
MAPE	0.04064	0.07112
MBE (MW)	44.01312	175.3006
KSIPer (%)	49.05248	145.6741
OVERPer (%)	0.37592	55.5244
SD (MW)	382.2192	609.539
Skewness	−0.21336	0.18288
Kurtosis	2.50952	3.4036
95th percentile (MW)	851.6823	1417.168
Capacity (MW)	6185.408	6185.408

3.2. Data selection

The data selection is carried out to increase the maximum applicability of RBNN and it allows the model reusability. In this regards, the

Table 2d
Metrics evaluated for next one year time period over 1000 solar plants using proposed RBNN.

Metrics	One hour-ahead	One-day ahead
Correlation coefficient	1.01092	1.00584
RMSE (MW)	1512.092	2754.691
NRMSE	0.02032	0.04064
MaxAE (MW)	16385.36	18265.17
MAE (MW)	1081.552	2005.482
MAPE	0.02032	0.03048
MBE (MW)	134.2441	1521.247
KSIPer (%)	48.52416	135.0467
OVERPer (%)	0.065416	42.09288
SD (MW)	1506.159	2296.251
Skewness	−0.23368	0.62992
Kurtosis	4.89712	3.82016
95th percentile (MW)	3128.589	5743.042
Capacity (MW)	65526.92	65526.92

study defines requirement set for the selection of components in a way that data is collected optimally. The model is trained and tested under various conditions and specifically for the purpose of training, various information are collected that includes: energy generated, solar factors, other atmospheric and geological factors and finally, the electrical factors post installation. After acquiring all the factors the study offers various outputs like installation size (kW), total energy generated per day basis (kWh/day) and ratio of energy conversion (%).

3.3. Feature extraction

The tokens present in the texts of the input PV plant dataset is converted to a components. It allows the representation of various embedding dimensions to extract the event trigger. Consider a set (v,h) from the pre-processed data item, where $E(v,h|\theta)$ is defined as an energy function that is utilised for training the feature selector in unsupervised manner and in addition the RBM uses the probability distribution function (PDF) to define the solutions.

Here, the energy function is defined as follows:

$$E(v,h|\theta) = -\sum_{i=1}^{n} a_i v_i - \sum_{j=1}^{m} b_i h_i - \sum_{i=1}^{n}\sum_{j=1}^{n} v_i w_{ij} h_j \tag{1}$$

where

θ is represented as the RBM parameter $\theta = \{W_{ij}, a_i, b_j\}$
w is represented as the weights of each layer, and
a is represented as the visible hidden layer bias and

Table 3
Comparison with other existing methods.

Metrics	1 solar plant		50 solar plants		100 solar plants		1000 solar plants	
	One hour-ahead	One-day ahead	One hour-ahead	One-day ahead	One hour-ahead	One-day ahead	One hour-ahead	One-day ahead
(a) DBN								
Correlation coefficient	0.784515	0.670966	0.970321	0.898063	0.990966	0.939353	1.027095	1.021933
RMSE (MW)	17.67222	22.78189	293.5323	452.3862	390.8637	644.3239	1536.286	2798.766
NRMSE	0.175484	0.227096	0.08258	0.134193	0.061935	0.103226	0.020645	0.04129
MaxAE (MW)	76.72759	86.81273	1346.815	2333.869	1791.212	3489.314	16647.52	18557.41
MAE (MW)	11.70578	15.28771	197.3364	295.8962	264.9698	426.4353	1098.857	2037.57
MAPE	0.113548	0.154838	0.061935	0.08258	0.04129	0.072258	0.020645	0.030968
MBE (MW)	2.260641	4.407733	32.66058	136.072	44.71733	178.1055	136.392	1545.587
KSIPer (%)	107.7882	223.7208	54.54441	190.2448	49.83732	148.0049	49.30055	137.2075
OVERPer (%)	29.06833	140.7584	0.794837	97.47593	0.381935	56.41279	0.066463	42.76637
SD (MW)	40.84637	22.34834	291.7362	431.483	388.3347	619.2917	1530.258	2332.991
Skewness	0.08258	−0.19613	−0.20645	0.206451	−0.21677	0.185806	−0.23742	0.639999
Kurtosis	2.477414	2.105802	2.601285	3.91225	2.549672	3.458058	4.975474	3.881283
95th percentile (MW)	40.84637	52.22183	658.0116	1022.615	865.3092	1439.842	3178.647	5834.93
Capacity (MW)	98.4252	98.405	3408.465	3408.465	5992.126	5992.126	63479.33	63479.33
(b) BPNN								
Correlation coefficient	0.802558	0.686399	0.992638	0.918718	1.013758	0.960958	1.050718	1.045438
RMSE (MW)	18.07868	23.30587	300.2836	462.7911	399.8536	659.1433	1571.621	2863.138
NRMSE	0.17952	0.23232	0.08448	0.13728	0.06336	0.1056	0.02112	0.04224
MaxAE (MW)	78.49232	88.80942	1377.792	2387.548	1832.41	3569.569	17030.42	18984.23
MAE (MW)	11.97502	15.63933	201.8751	302.7018	271.0641	436.2433	1124.131	2084.434
MAPE	0.11616	0.1584	0.06336	0.08448	0.04224	0.07392	0.02112	0.03168
MBE (MW)	2.312635	4.509111	33.41177	139.2016	45.74583	182.2019	139.529	1581.135
KSIPer (%)	110.2673	228.8664	55.79893	194.6204	50.98358	151.409	50.43446	140.3632
OVERPer (%)	29.7369	143.9959	0.813118	99.71788	0.390719	57.71028	0.067991	43.74999
SD (MW)	41.78584	22.86235	298.4461	441.4071	397.2664	633.5354	1565.454	2386.65
Skewness	0.08448	−0.20064	−0.2112	0.2112	−0.22176	0.19008	−0.24288	0.654719
Kurtosis	2.534395	2.154236	2.661115	4.002232	2.608315	3.537593	5.08991	3.970552
95th percentile (MW)	41.78584	53.42293	673.1459	1046.135	885.2113	1472.959	3251.755	5969.134
Capacity (MW)	84.84931	84.84931	2938.332	2938.332	5165.626	5165.626	54723.56	54723.56
(c) ANN								
Correlation coefficient	0.830086	0.709942	1.026685	0.95023	1.04853	0.993919	1.086758	1.081296
RMSE (MW)	18.69878	24.10526	310.5833	478.6648	413.5686	681.7519	1625.527	2961.343
NRMSE	0.185677	0.240288	0.087377	0.141988	0.065533	0.109222	0.021844	0.043689
MaxAE (MW)	81.18461	91.85559	1425.05	2469.441	1895.261	3692.005	17614.56	19635.39
MAE (MW)	12.38576	16.17576	208.7994	313.0845	280.3616	451.2064	1162.689	2155.93
MAPE	0.120,144	0.163,833	0.065533	0.087377	0.043689	0.076455	0.021844	0.032,767
MBE (MW)	2.391959	4.663773	34.5578	143.9763	47.31491	188.4514	144.3148	1635.368
KSIPer (%)	114.0495	236.7165	57.71283	201.2959	52.73231	156.6023	52.16436	145.1777
OVERPer (%)	30.75688	148.9349	0.841008	103.1382	0.404121	59.68975	0.070323	45.25062
SD (MW)	43.21909	23.64653	308.6828	456.5474	410.8926	655.2656	1619.149	2468.512
Skewness	0.087377	−0.20752	−0.21844	0.218444	−0.22937	0.196599	−0.25121	0.677176
Kurtosis	2.621325	2.228126	2.752391	4.139509	2.69778	3.658932	5.264494	4.106742
95th percentile (MW)	43.21909	55.25534	696.2348	1082.017	915.5741	1523.481	3363.291	6173.875
Capacity (MW)	78.80581	78.80581	2729.045	2729.045	4797.698	4797.698	50825.81	50825.81

b is represented as the hidden layer bias.

The joint PDF between the output and hidden layer (h), which is solely expressed as below:

$$P(v,h|\theta) = \frac{e^{-E(v,h|\theta)}}{Z(\theta)} \tag{2}$$

$$Z(\theta) = \sum_{v,h} e^{-E(v,h|\theta)} \tag{3}$$

The conditional PDF between the hidden layers is expressed in the form of Gibbs sampling function:

$$P(h_j = 1|v,\theta) = sigmoid\left(b_j + \sum_i v_i w_{ij}\right) \tag{4}$$

$$P(v_j = 1|v,\theta) = sigmoid\left(a_j + \sum_i h_i w_{ji}\right) \tag{5}$$

Using Eq. (3), the joint PDF of hidden layer is derived in an active state. Now the RBM feature extractor points out the symmetric feature in the activation state of a and h, where the probability of activation state is determined by Eq. (4).

3.4. Prediction

The unsupervised feature learning process obtains the corresponding RBM weight w and it train iteratively the RBM to acquire the entire weights $W = w_1, w_2 \ldots w_l$. Finally, the connection weights are fine tined with supervised BP learning from unsupervised RBM learning. The supervised learning enables the determination of gradient through the training data label and accordingly adjusts the parameters in the network. Finally, a minimal prediction error or prediction error is obtained using the RBNN.

RBNN is uses RBM for feature extraction and BPNN for classification of the energy generation from the PV array modules. The Fig. 2 shows the structure of training-testing RBNN network, which has stacked Restrict Boltzmann Machines (RBM) and a BPNN classifier for PV energy generation prediction in its deep network.

To achieve this, the study uses two different models, where RBM acts in an unsupervised way to learn the features related to PV plants and BPNN acts in a supervised way to classify the features for the prediction of its performance. The study uses RL algorithm to provide feedback of the results obtained at each iterations, where these feedback would enable the model to predict accurately by restricting the errors while prediction of the performance of PV plants. The RL algorithm provides action (either award or penalty) based on the features extracted by the RBM feature extractor. Depending on the features selected, the RL defines certain rules in association with a similarity comparison module, which checks the classification accuracy of BPNN based on these rules.

3.5. Rule set

The RL defines the set of rules based on the features extracted by the RBM and it helps in classification of features using BPNN, when the rules are been fed into the similarity comparison unit of the prediction unit. The rules are specified as the IF-THEN rules that enables network being described with decentralized information. The prediction rule over each class label is extracted using the following manner,

$$\begin{aligned} R_i : IF&\left(x_{s1} > V_1 \ or \ x_{s1} < V_1^{'}\right) \\ &\wedge \left(x_{s2} > V_2 \ or \ x_{s2} < V_2^{'}\right) \wedge \ldots \\ &\wedge \left(x_{sn} > V_n \ or \ x_{sn} < V_n^{'}\right) \ then \ y = c \end{aligned} \tag{6}$$

where

R_j is defined as the rules allocated for each feature label,

$(x_{s1}, x_{s2},\ldots,x_{sn})$ is defined as the rule elements of each feature label,

V is defined as the real values learnt by the BPNN,

y is defined as label for a specific class c.

For classification of the extracted features, the study develops rules for prediction of instances. The rules defines the relationship between the class labels and the prediction events, which spontaneously reduces the classification error. The classification rule defined by the RL algorithm is generally evaluated by the fitness function:

$$Fitness = \frac{\left(\frac{TP}{(TP+FN)}\right)}{\left(\frac{TN}{(FP+TN)}\right)} \tag{7}$$

Where,

TP - True Positive;

TN - True Negative;

FP - False Positive;

FN - False Negative;

Thus for each PV prediction rule, the study uses following metrics to evaluate its effectiveness:

$$\text{Sensitivity} = \frac{TP}{TP + FN}$$

$$\text{Specificity} = \frac{TN}{FP + TN}.$$

Algorithm for Prediction using RBNN

```
For i = 1:N forecast horizons do
    Filter the data depending on the solar availability;
    Eliminate the redundant observations;
    Partition the training and testing dataset;
    Partition training data into k half-year folds;
    Define a component or parameter set;
    For each component p in the input component do
        For each i in set of K folds do
            Use i as validation set;
            Pre-process the solar data;
            Fit RBNN;
            Predict test set values;
        End
        Calculate RMSE on test sets;
    End
    Determine hyper-parameters:
        Nodes per layer (10);
        Weight decay (0.01);
        Hidden layers (3)
    Train the model with optimal hyper-parameters;
    Evaluate the test set from RBNN model;
End
```

4. Results and discussions

In this section, the prediction of energy generation performance using the RBNN classifier is estimated in terms of various other classifiers. The RBNN combined with RL is evaluated with various other algorithms that includes: Artificial Neural Network (ANN), BPNN and Deep Belief Network (DBN). The proposed RBNN integrates the RBM with BPNN, it is hence essential to test the performance of BPNN algorithm over the dataset used. The novel solution using RBNN urges the model to compare itself with DBN and ANN, since these model acts as an ancestor to the proposed novel solution. Comparison with all these three neural network model would enable the study to define the efficacy of the RBNN. Also, the difference between the existing and the proposed solution is that the RBNN integrates BPNN and RL for different tasks, however the conventional model fails to do so.

In general, the study is tested with all the error metrics to check if the study reports increased accuracy and also the study aims to report how well the model abide with a given dataset. The proposed method is tested against various performance measures that includes Root mean squared error (RMSE), normalized root mean squared error (NRMSE), mean bias error (MBE), Mean absolute error (MAE), Maximum absolute error (MaxAE), mean absolute percentage error (MAPE), Kolmogorov–Smirnov test integral (KSI) and OVER metrics, Skewness and kurtosis and variability estimation metrics that includes: forecast errors and varying geographic locations.

$$RMSE = \sqrt{\frac{\sum_{i=1}^{n}\left(Y(i) - \widehat{Y}(i)\right)^2}{N}} \tag{8}$$

Where

$Y(i)$ is the actual generated PV output and

$\widehat{Y}(i)$ is the predicted PV output.

N is the total estimated points in forecasting time period.

$$nRMSE = \frac{1}{\max(Y)}\sqrt{\frac{\sum_{i=1}^{n}\left(Y(i) - \widehat{Y}(i)\right)^2}{N}} \tag{9}$$

$$MaxAE = \max\left|Y(i) - \widehat{Y}(i)\right| \tag{10}$$

$$MAE = \frac{1}{N}\sum_{i=1}^{N}\left|Y(i) - \widehat{Y}(i)\right| \tag{11}$$

$$MAPE = \frac{1}{N}\sum_{i=1}^{N}\left|\frac{Y(i) - \widehat{Y}(i)}{Capacity}\right| \tag{12}$$

where *Capacity* – capacity of each PV array for power generation

$$MBE = \frac{1}{N}\sum_{i=1}^{N}\left(\widehat{Y}(i) - Y(i)\right) \tag{13}$$

$$D = \max\left|F(i) - \widehat{F}(i)\right| \tag{14}$$

where,

$F(i)$ is the CDF of the actual generated PV output and

$\widehat{F}(i)$ is the CDF of the predicted PV output.

$$KSI(\%) = \frac{\int_{p_{\min}}^{p_{\max}} D_n dp}{a_c} \times 100 \tag{15}$$

$$OVER(\%) = \frac{\int_{p_{\min}}^{p_{\max}} t dp}{a_c} \times 100 \tag{16}$$

$$\text{Skewness}: \gamma = E\left[\left(\frac{e - \mu_e}{\sigma_e}\right)^3\right] \tag{17}$$

Where,

γ is defined as the skewness;

e is defined as the forecast error

μ_e is defined as the mean of forecast error

σ_e is defined as the standard deviation of the forecast error

$$\text{Kurtosis}: \kappa = \left(\frac{\mu_4}{\sigma_e^4}\right) - 3 \tag{18}$$

Where,

μ_4 is defined as the mean of fourth moment

σ_e is defined as the standard deviation of the forecast error

$$\text{Variability Estimation } f(x;h) = \frac{1}{n}\sum_{i=1}^{n} K_h(x - x(i)) \tag{19}$$

The data is obtained from [26] and the investigations are carried out at one hour-ahead and Day-ahead solar forecast errors. The specifications used for the study is given in Table 1.

Tables 2a–2d shows the metrics evaluated for next one year time period over a solar plant, 50 solar plants, 100 solar plants and 1000 solar plants during validation. The results over various metrics shows that the prediction error is less in one hour ahead and one-day ahead validation. The results further shows that the proposed method has reduced prediction errors with maximal prediction accuracy than other methods (as in Table 3).

5. Conclusions

In this paper, RBNN studies large set of features from the input data during the process of feature extraction and classification. The RL further enhances the generation of rules for predicting the optimal energy output from the PV plant based on various input features or components. The study provides an improved response rate than other methods using its RBM and BPNN. The BPNN performance boosted by the RL rule set generation improves the rate of prediction. The results of simulation shows that the rate of prediction is improved in BPNN than other classifiers with its event modelling and shows reduced prediction error than other methods. The results of multiple metrics thus successfully evaluates the solar forecast quality based on its input to the RL. However, under-forecast is detected at some point of observation, especially in one hour ahead forecasting. The sensitivity of the RBNN shows improved forecast or sensitivity over other methods in terms of its uniformity, skewness and kurtosis metrics. In future, the combination of wind farms may be considered for evolution over various metrics.

Author statement

We have submitted our revised version of our manuscript by addressing all the comments suggested by the reviewers for the special issue, I am confirming on behalf of all my coauthors I have not submitted this article anywhere, also if any further improvisation to be made we are ready to work on it.

Declaration of Competing Interest

There no conflict of interest for this article.

References

[1] O. Abedinia, N. Amjady, N. Ghadimi, Solar energy forecasting based on hybrid neural network and improved metaheuristic algorithm, Comput. Intell. 34 (1) (2018) 241–260.
[2] L.M. Aguiar, B. Pereira, P. Lauret, F. Díaz, M. David, Combining solar irradiance measurements, satellite-derived data and a numerical weather prediction model to improve intra-day solar forecasting, Renew. Energy 97 (2016) 599–610.
[3] L. Bao, X. Sun, Y. Chen, D. Gong, Y. Zhang, Restricted boltzmann machine-driven interactive estimation of distribution algorithm for personalized search, Knowledge Based Syst. (2020), 106030.

[4] J.M. Barrera, A. Reina, A. Maté, J.C. Trujillo, Solar energy prediction model based on artificial neural networks and open data, Sustainability 12 (17) (2020) 6915.
[5] J. Chen, J. Yu, M. Song, V. Valdmanis, Factor decomposition and prediction of solar energy consumption in the United States, J. Clean. Prod. 234 (2019) 1210–1220.
[6] S. Chen, Y. Zhao, Y. Bie, The prediction analysis of properties of recycled aggregate permeable concrete based on back-propagation neural network, J. Clean. Prod. 276 (2020), 124187.
[7] Z. Chen, H. Hu, Y. Wu, Y. Zhang, G. Li, Y. Liu, Stochastic model predictive control for energy management of power-split plug-in hybrid electric vehicles based on reinforcement learning, Energy 211 (2020), 118931.
[8] Z. Chen, W. Ma, W. Dai, W. Pan, Z. Ming, Conditional restricted Boltzmann machine for item recommendation, Neurocomputing 385 (2020) 269–277.
[9] N. Dong, J.F. Chang, A.G. Wu, Z.K. Gao, A novel convolutional neural network framework based solar irradiance prediction method, Int. J. Electr. Power Energy Syst. 114 (2020), 105411.
[10] Y.Q. Feng, Y.Z. Liu, X. Wang, Z.X. He, T.C. Hung, Q. Wang, H. Xi, Performance prediction and optimization of an organic Rankine cycle (ORC) for waste heat recovery using back propagation neural network, Energy Convers. Manage. 226 (2020), 113552.
[11] J. Ferrero Bermejo, J.F. Gomez Fernandez, F. Olivencia Polo, A. Crespo Márquez, A review of the use of artificial neural network models for energy and reliability prediction. A study of the solar PV, hydraulic and wind energy sources, Appl. Sci. 9 (9) (2019) 1844.
[12] P. Fitriaty, Z. Shen, Predicting energy generation from residential building attached Photovoltaic Cells in a tropical area using 3D modeling analysis, J. Clean. Prod. 195 (2018) 1422–1436.
[13] B. Ghazanfari, F. Afghah, M.E. Taylor, Sequential association rule mining for autonomously extracting hierarchical task structures in reinforcement learning, IEEE Access 8 (2020) 11782–11799.
[14] L.M. Halabi, S. Mekhilef, M. Hossain, Performance evaluation of hybrid adaptive neuro-fuzzy inference system models for predicting monthly global solar radiation, Appl. Energy 213 (2018) 247–261.
[15] https://www.kaggle.com/anikannal/solar-power-generation-data?select=Plant_1_Weather_Sensor_Data.csv.
[16] M.H. Huang, R. Rust, V. Maksimovic, The feeling economy: managing in the next generation of artificial intelligence (AI), Calif. Manage. Rev. 61 (4) (2019) 43–65.
[17] H.A. Kazem, J.H. Yousif, M.T. Chaichan, Modeling of daily solar energy system prediction using support vector machine for Oman, Int. J. Appl. Eng. Res. Dev. 11 (20) (2016) 10166–10172.
[18] J.G. Kim, D.H. Kim, W.S. Yoo, J.Y. Lee, Y.B. Kim, Daily prediction of solar power generation based on weather forecast information in Korea, Iet Renew. Power Gener. 11 (10) (2017) 1268–1273.
[19] S. Kosunalp, A new energy prediction algorithm for energy-harvesting wireless sensor networks with Q-learning, IEEE Access 4 (2016) 5755–5763.
[20] D. Lee, A.M. Arigi, J. Kim, Algorithm for autonomous power-increase operation using deep reinforcement learning and a rule-based system, IEEE Access 8 (2020) 196727–196746.
[21] K.B. Letaief, W. Chen, Y. Shi, J. Zhang, Y.J.A. Zhang, The roadmap to 6G: AI empowered wireless networks, IEEE Commun. Mag. 57 (8) (2019) 84–90.
[22] Y. Liu, H. Qin, Z. Zhang, S. Pei, C. Wang, X. Yu, et al., Ensemble spatiotemporal forecasting of solar irradiation using variational Bayesian convolutional gate recurrent unit network, Appl. Energy 253 (2019), 113596.
[23] S.M. Mousavi, E.S. Mostafavi, P. Jiao, Next generation prediction model for daily solar radiation on horizontal surface using a hybrid neural network and simulated annealing method, Energy Convers. Manage. 153 (2017) 671–682.
[24] S. Pirmoradi, M. Teshnehlab, N. Zarghami, A. Sharifi, The self-organizing restricted boltzmann machine for deep representation with the application on classification problems, Expert Syst. Appl. 149 (2020), 113286.
[25] X. Qing, Y. Niu, Hourly day-ahead solar irradiance prediction using weather forecasts by LSTM, Energy 148 (2018) 461–468.
[26] F. Rodríguez, A. Fleetwood, A. Galarza, L. Fontán, Predicting solar energy generation through artificial neural networks using weather forecasts for microgrid control, Renew. Energy 126 (2018) 855–864.
[27] W. Sun, C. Huang, A carbon price prediction model based on secondary decomposition algorithm and optimized back propagation neural network, J. Clean. Prod. 243 (2020), 118671.
[28] J. Xu, L. Yao, L. Li, M. Ji, G. Tang, Argumentation based reinforcement learning for meta-knowledge extraction, Inf. Sci. 506 (2020) 258–272.
[29] J.M. Yeom, R.C. Deo, J.F. Adamwoski, T. Chae, D.S. Kim, K.S. Han, D.Y. Kim, Exploring solar and wind energy resources in North Korea with COMS MI geostationary satellite data coupled with numerical weather prediction reanalysis variables, Renew. Sustain. Energy Rev. 119 (2020), 109570.
[30] R.H.M. Zargar, M.H.Y. Moghaddam, Development of a Markov-Chain-Based solar generation model for smart microgrid energy management system, IEEE Trans. Sustain. Energy 11 (2) (2019) 736–745.